4.6 REAR-INFLOW EVOLUTION IN A NON-SEVERE BOW-ECHO OBSERVED BY AIRBORNE DOPPLER RADAR DURING BAMEX

David P. Jorgensen*
NOAA/National Severe Storms Laboratory
Norman, Oklahoma

Hanne V. Murphey and Roger M. Wakimoto
University of California, Los Angeles
Los Angeles, California

1. INTRODUCTION

The Bow-Echo and Mesoscale Convective Vortex Experiment (BAMEX) collected specialized observations, using highly mobile platforms, within bow-echo mesoscale convective systems in the Midwest U.S. The field exercise ran during the late spring/early summer of 2003 from a main base of operations at MidAmerica Airport near St. Louis, MO. BAMEX has two principal foci: 1) improve understanding and improve prediction of bow echoes (Fujita 1978), principally those which produce damaging surface winds and last at least 4 hours and (2) document the mesoscale processes which produce long lived mesoscale convective vortices (MCVs). More information concerning the science objectives and the observational strategies of BAMEX are contained in the scientific overview document: http://www.mmm.ucar.edu/bamex/science.html.

Primary mobile platforms and instruments deployed for BAMEX include two turboprop P-3s operated by NOAA and the Naval Research Laboratory (NRL) that were equipped with vertically-scanning X-band Doppler radars (Jorgensen et al. 1983), a leased Lear-34 for dropsonde deployments, and the mobile integrated profiling system (MIPS) operated by the University of Alabama-Huntsville. The NRL aircraft carried the ELDORA radar provided by the National Center for Atmospheric Research (NCAR) (Hildebrand et al 1996). During the approximately 50 day field campaign, 18 total Intensive Observation Periods (IOPs) were obtained, 9 of which observed at least a part of the life cycle of a bow echo.

A more complete description of the BAMEX IOPs, including data set availability, can be found on the University Corporation for Atmospheric Research/Joint Office for Science Support (UCAR/JOSS) projects catalog web site: http://www.joss.ucar.edu/bamex/catalog/.

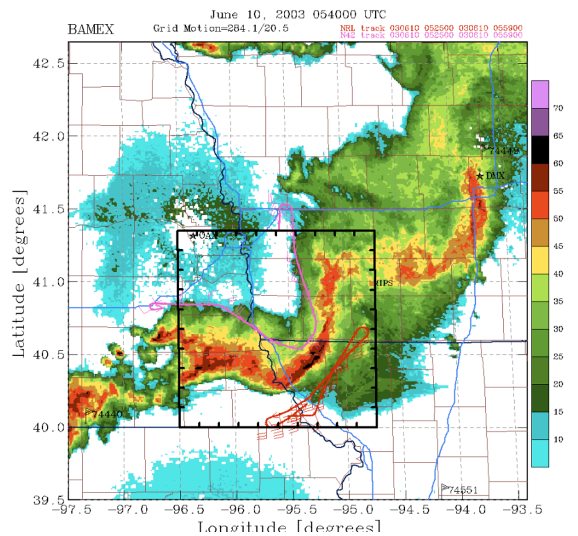

Fig. 1. Composite National Weather Service WSR-88D base reflectivity at 0540 UTC 10 June 2003. WSR-88D radars are indicated by the stars, profilers by the flags, solid black lines are state boundaries, light brown lines are county boundaries, blue lines are interstate highways. Flight tracks for the two turbo prop aircraft are red lines (NRL P-3) and magenta lines (NOAA P-3). The aircraft tracks were adjusted by the convective line speed of from 284 degrees at 20.5 m s^{-1} to correspond to the radar composite time. The heavy black box with tic marks shows the location of the pseudo-dual-Doppler analysis region.

One such mission on 10 June 2003 (IOP7) investigated a rapidly moving bow-echo system for nearly 6 hours. In spite of the impressive bow-shaped structure on radar (Fig. 1) and the strong mid-level rear inflow jet of ~40 m s^{-1} relative to the ground (to be discussed) the surface winds during the time of aircraft investigation were surprisingly weak. Evening soundings indicated the region of MO-IA-KS-NB to be highly conditionally unstable with Convective Available Potential Energy (CAPE) ~1000-3000 J kg^{-1} with the lower level (0-1.5 km) wind shear > 20 m s^{-1}, possibly indicating

*Corresponding author address: David P. Jorgensen, NOAA/National Severe Storms Laboratory, Norman, OK 73069; e-mail: David.P.Jorgensen@noaa.gov.

conditions favorable for bow echoes or even derechoes (Johns and Hirt 1987; Johns 1993).

2. DATA

The data used in this study was the airborne Doppler radar data collected by the NOAA P-3 and Eldora on the NRL P-3. For many of the bow-echo passes obtained during BAMEX, the aircraft were synchronized such that their leg start times were within a few minutes of each other and their respective tail-radar beam patterns overlapped the area of interest (usually the convective line). In all but one IOP the NRL was on the "front" side of the convective line and the NOAA P-3 on the "rear" or stratiform rain side. In addition to the Doppler radar data collected, the NOAA P-3 usually performed several spiral descents within the strongest rear inflow notches to collect microphysical data sets that will help infer the role that raindrop evaporative cooling plays in help drive high momentum air downwards.

The Doppler radar data was edited for 2nd trip ground clutter and other artifacts (e.g., processor dealiasing mistakes) using NCAR's SOLO software (Oye et al. 1996). Very little dealiasing of the data was required as the signal processor systems on both radars employed the staggered PRF technique for extending the Nyquist intervals to >50 m s^{-1} (Jorgensen et al. 2000).

Once cleaned up, the Doppler data from both aircraft were interpolated to common Cartesian grids with a spacing $\Delta x=\Delta y=1.5$ km and $\Delta z=0.5$ km. The vertical grid levels were constructed relative to mean sea level (MSL). Ground return was removed using a high-resolution digital topographic data set. Vertical velocity was estimated from vertical integration of horizontal divergence estimates. For the quad-Doppler legs the vertical velocity at echo top was directly measured and used to start the downward divergence integration. An O'Brien (1970) divergence correction was made to the vertical column to insure that *w*=0 at the ground. For non-quad legs w=0 at echo top was assumed. A two-step Leise filter (Leise 1981) was applied to the velocity data prior to computation of the vertical velocity to remove artifacts of wavelength less that about 4Δx and to retain greater than 90% of the energy of features with wavelength >8Δx.

The maximum range of the radars is about 45 km, which implies a maximum time displacement between fore and aft scans of about 4 minutes. During that time, as well as for the duration of each flight leg that comprises the complete volume scan, the weather within the analysis domain is assumed to be "stationary". Stationarity over the 4-10 minutes required to complete the volume scan is a fairly common assumption for airborne and ground-based Doppler radar studies. Nevertheless, this assumption is a limiting factor in interpreting the data collected on relatively quickly evolving systems, such as individual convective storm cells. The larger, more mesoscale, structure of the bow-echo system is more resolvable with this type of Doppler radar data.

For the analyses presented here, eight time periods were examined from about 0416 UTC to 0740 UTC. Table 1 shows the characteristics of these flight legs. The last six legs are suitable for quad-Doppler analysis, although the 0510 UTC time had a fairly long gap (20.5 min) between the two flight legs, which increases the uncertainty of the analysis.

Table 1. Flight legs used in the study. The last column (Δt) is the time difference (minutes) between the mid-point times of the two aircraft legs.

Analysis Time (UTC)	NOAA P-3 start-end	NRL P-3 start-end	Δt (min)
0430	0416-0437	n/a	-
0450	0439-0458	n/a	-
0510	0500-0525	0528-0538	20.5
0540	0529-0600	0539-0553	1.5
0610	0600-0617	0605-0620	4.0
0630	0617-0636	0622-0629	1.0
0650	0636-0657	0640-0657	2.0
0750	0740-0752	0744-0808	10.0

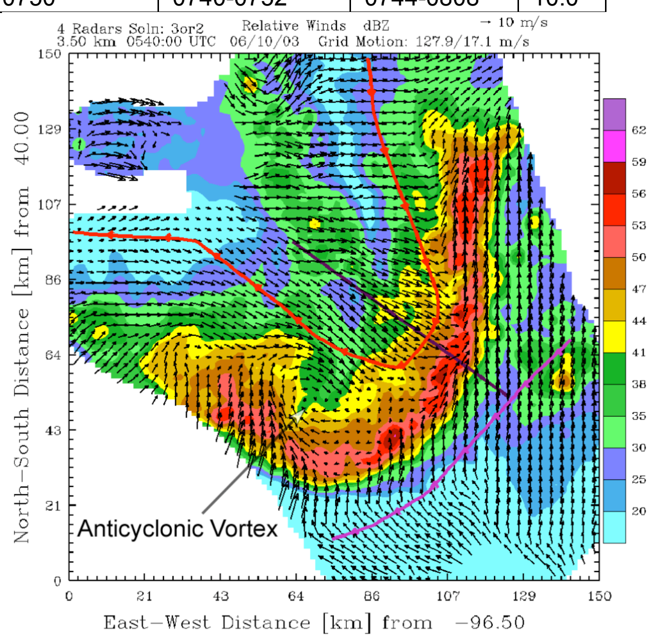

Fig. 2. Horizontal Doppler-derived winds and reflectivity at 3.5 km MSL from the quad-Doppler analysis. Flight tracks are the red (NOAA P-3) and purple (NRL P-3) solid lines. The black line shows the location of a vertical cross section shown in Fig. 3.

3. BASIC STRUCTURE OF THE BOW-ECHO SYSTEM

The 0540 UTC analysis time is used to illustrate the horizontal structure and flow fields. Fig. 2 depicts the reflectivity and storm-relative horizontal flow field at 3.5 km.

The dominant features of Fig. 2 is the presence of a pronounced anticyclonic "bookend"-type vortex near the cusp of the bow and a strong rear-inflow jet directed at the apex of the bow, both features reminiscent of modeled bow-echo storms (Weisman and Davis 1998). Lack of a corresponding cyclonic vortex on the northern side of bow is somewhat surprising given the strength of the rear-inflow jet and the pronounced curvature of the bow. However, the larger scale structure of the echo (Fig. 1) shows that to the northeast of the bow under study was another bow-echo system. We speculate that the line-end vortices of the two systems may have counteracted each other.

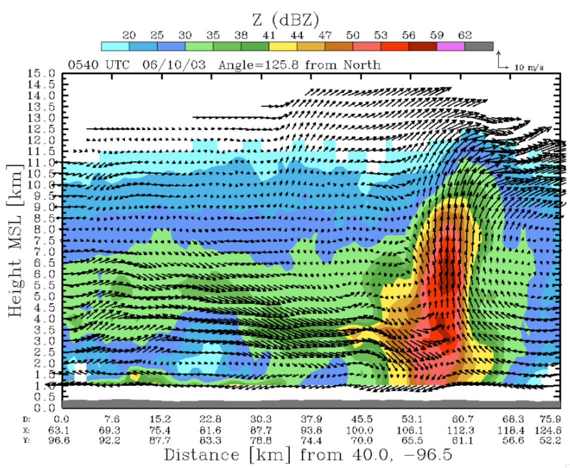

Fig. 3. Vertical cross section of reflectivity and storm-relative winds approximately normal to the orientation of the leading convective line. The location is shown as the dark line in Fig. 2. The vertical axis is height relative to MSL, so the topography (derived from a high-resolution digital data base) is shown as the gray area near the bottom. The vector scale (shown in the upper right) is vertically stretched to match the aspect ratio of the plot.

A vertical cross section of reflectivity and storm-relative wind is shown in Fig. 3. A nearly vertically erect updraft and reflectivity core is seen, although other cross sections at difference locations along the convective line show upshear or downshear tilted updraft cores, perhaps indicative of horizontal variability in cold-pool strength and/or low-level environmental shear in light of RKW theory (Rotunno et al. 1988). A strong rear inflow is also seen that descends as it approaches the convective line. The lowest information level is about 500-700 m above the terrain due to the fairly conservative nature of the ground removal algorithm which deletes radar gates if the bottom of the beam gets closer that about 100 m of the surface. Surface observations confirmed that there were no strong surface winds observed with the passage of this event.

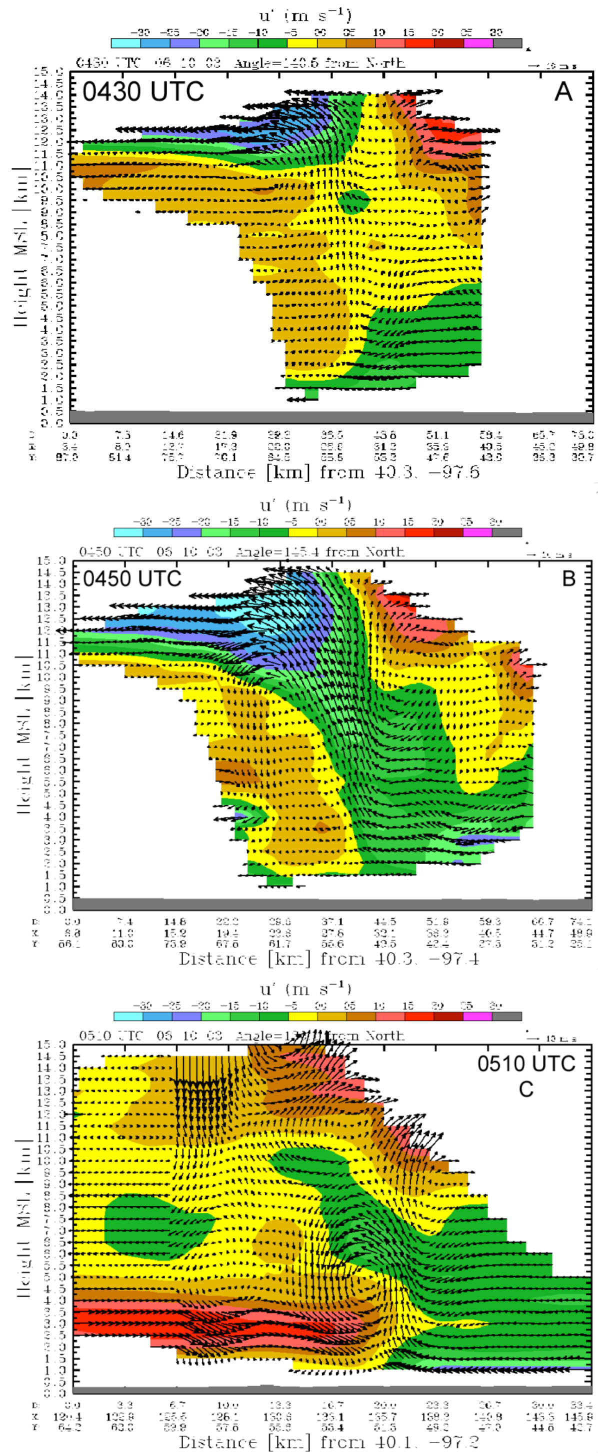

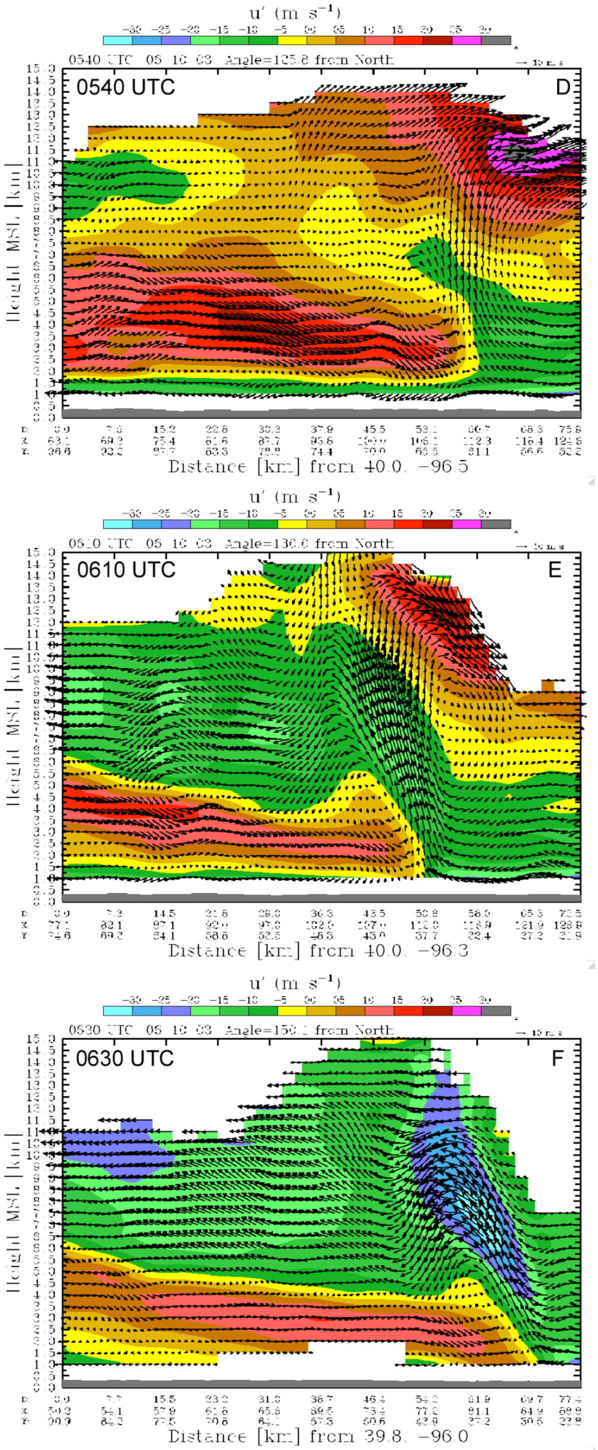

4. REAR-INFLOW EVOLUTION

The evolution of the storm-relative rear inflow is shown in a series of vertical cross sections of line-relative flow in Fig. 4. The cross sections were chosen to be approximately normal to the orientation of the leading convective line, and roughly in the same location near the apex of the bow. In the two earliest time periods (Fig. 4a & 4b, 0430 UTC & 0450 UTC, respectively) the system was in an organization phase and the rear inflow was fairly

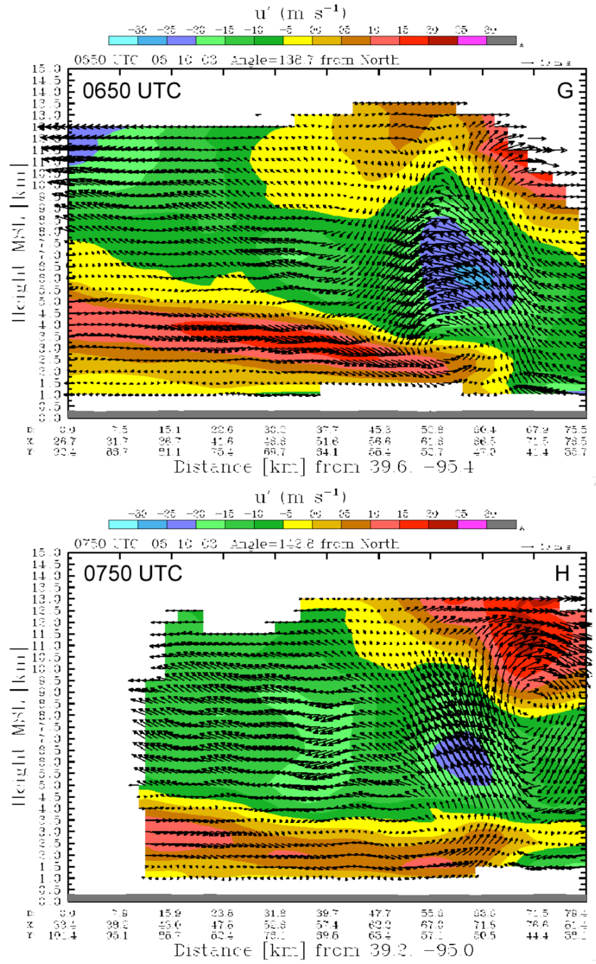

Fig. 4. Vertical cross sections of Doppler-derived storm-relative flow in the plane of the cross section for 7 time periods (A:0430 UTC; B:0450 UTC; C:0510 UTC; D:0540 UTC; E:0610 UTC; F: 0630 UTC; G:0650 UTC; H:0750 UTC). Color scale (m s^{-1}) is at the top of each figure. Negative velocities (yellow, green, and blue colors) recede from the convective line while positive velocities (brown, red, and magenta colors) approach the line. Vectors are stretched vertically as in Fig. 3. Horizontal distance is ~75 km in all plots.

weak with no distinct jet-like feature. These time periods were also before the commencement of the quad-Doppler patterns so the areal coverage of the convective line was reduced. A dramatic change in the rear-inflow structure occurred by 0510 UTC (Fig. 4c) with a jet-like structure appearing with the core near 3 km MSL and maximum inflow strength of 15-20 m s^{-1}. The 0510 UTC analysis was the one that involved a time difference between the NOAA and NRL P-3 leg times of over 20 minutes (Table 1). Therefore, the vertical velocity vectors in the Fig. 4c (0510 UTC) plot, particularly near the echo top, are suspect. The horizontal winds in the rear inflow region were derived primarily from the nearby NOAA P-3 data and should be fine.

By the 0540 UTC quad passes (Fig. 4d) the jet had strengthened to over 20 m s^{-1} and was showing signs of descending toward the convective line. Below the jet axis near 4 km MSL the jet flow weakened, eventually returning to front-to-rear flow at the lowest levels (~1 km MSL or about 700 m AGL) detectable by the airborne radars. The front-to-rear flow continued to descend, but not strengthen significantly, in the 0610 UTC pass (Fig. 4e). Strengthening of the front-to-rear flow at mid-levels in the vicinity of the convective line was evident in the 0630 UTC quad passes (Fig. 4f), yet the rear inflow showed weakening and continued descent. The 0650 UTC pass (Fig. 4g) revealed a minor strengthening of the rear inflow to perhaps ~15 m s^{-1} in the core axis, however by the final quad pass at 0750 UTC (Fig. 4h), the jet had weakened to ~10 m s^{-1} and had become quasi-horizontal with the nose of the rear-inflow now ahead of the convective line and undercutting the primary leading line updraft.

In addition to the Doppler-derived winds indicating the strength of the rear-inflow jet, an independent estimate was provided by the NOAA P-3 flight levels winds at 3 km MSL during the many passes to the rear of the convective line. Those winds exceeded 40 m s^{-1} which compares favorably to the Doppler-derived storm-relative winds of ~20-25 m s^{-1}. Line motion during that pass was 17.3 m s^{-1} so ground-relative winds were >40 m s^{-1}.

5. SURFACE WINDS

In spite of the impressive bow-shaped structure on radar imagery and storm relative rear-inflow jet magnitudes of ~20-25 m s^{-1}, there were no strong surface wind reports from this system during the period of aircraft investigation. In fact, there were no *Storm Data* reports or significant wind gusts in the hourly SAO observations. There is evidence that strong rear inflow jets can descend to the surface and contribute to straight-line wind damage from bow-echo (and longer-lived derecho systems) (John and Hirt 1987; Johns 1993). However, damaging winds can also occur in conjunction with individual rotating cells and tornadoes along the leading edge (Tessendoff and Trapp 2000). This case apparently lacked either of these two processes. One potential clue to the reason the rear the rear inflow didn't penetrate to the surface may be evident in the soundings collected ahead of the system.

The 0000 UTC 10 June 2003 NWS sounding from Topeka (TOP) Kansas is shown in Fig. 5. At 0000 UTC TOP was approximately 225 km southeast of the developing bow echo. The sounding showed considerable convective instability (CAPE near 1000 J kg^{-1}). An inversion from about 850 mb to near 700 mb, indicative perhaps of subsidence, was evident and perhaps acted as a convective inhibitor in spite of the very warm surface conditions.

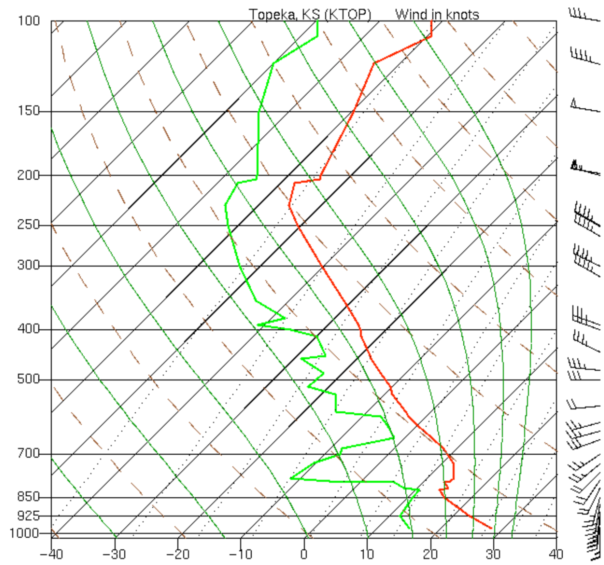

Fig. 5. SkewT-LogP plot of Topeka (TOP) sounding at 0000 UTC 10 June 2003. The red trace is the air temperature, the green trace dewpoint temperature.

By 0349 UTC, however, two dropsondes deployed by the Lear-34 very near TOP revealed substantially different near surface conditions (Fig. 6). In both drops, approximately 100 km apart, there has been substantial overturning of the lower 3 km layer from about 700 mb downward. Substantial stabilization has occurred, e.g., approximately the 730 mb level warmed several degrees C while the near surface temperature dropped by nearly 6 C. The layer from just above the surface to 700 mb has also moistened appreciably. While nocturnal cooling could be expected to lower the near surface temperature a few degrees, the warming above 925 mb, and the moistening, implies some larger-scale advective process was acting in addition to the normal diabatic nocturnal cooling. We speculate that this stabilization of the layer below 700 mb could have help reduce the penetration of rear-inflow air down toward the surface and lessoned chance of strong straight-line winds.

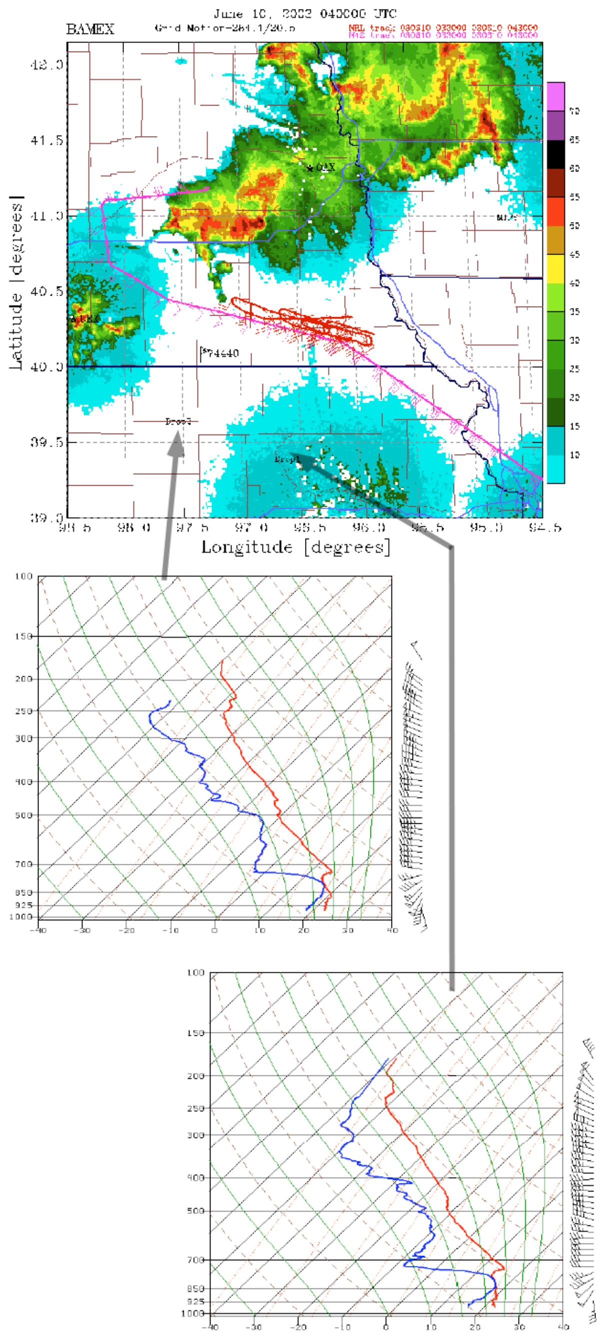

Fig. 6. As in Fig. 1 (top panel) except for 0400 UTC 10 June 2003. SkewT-logP plots of two dropsondes deployed by Lear-34 on the front side of the bow-echo system at 0349 UTC and 0357 UTC (bottom two panels with arrows indicating the locations of the drops). The red traces on the skewT-logP plots are the air temperature. Dewpoint temperatures are indicated by the blue lines.

Substantially more analysis and possibly numerical simulation of this bow-echo system will have to be done to prove the hypothesis that lower level stabilization can effect the downward movement of westerly momentum carried by the rear inflow jet. We plan to continue the analysis of Doppler and dropsonde data sets to explore this, and other, ideas as to why this system did not produce the expected surface winds.

Acknowledgments. We would like to the flight crews of the NOAA P-3, NRL P-3, and Lear-34 aircraft for their dedicated support in the execution of often hazardous flight patterns. The sounding data was supplied by the UCAR/JOSS web site. Lastly, we thank Dr. John Daugherty for his tireless efforts in managing the NOAA P-3 aircraft data sets.

References

Fujita, T. T., 1978: Manual of downburst identification for project NIMROD. Satellite and Mesometeorology Research Paper No. 156, Department of Geophysical Sciences, University of Chicago, 104 pp.

Hildebrand, Peter H., Lee, Wen-Chau, Walther, Craig A., Frush, Charles, Randall, Mitchell, Loew, Eric, Neitzel, Richard, Parsons, Richard, Testud, Jacques, Baudin, François, LeCornec, Alain. 1996: The ELDORA/ASTRAIA Airborne Doppler Weather Radar: High-Resolution Observations from TOGA COARE. *Bull. Amer. Meteor. Soc*., **77**, 213–232.

Johns, R.H., 1993: Meteorological conditions associated with bow echo development in convective storms. *Wea. Forecasting*, **8**, 294-299.

Johns, R.H. and W.D. Hirt, 1987: Derechos: widespread convectively induced windstorms. *Wea. Forecasting*, **2**, 32—49.

Jorgensen, D. P., P. H. Hildebrand, and C. L. Frush, 1983: Feasibility test of an airborne pulse-Doppler meteorological radar. *J. Climate Appl. Meteor*., **22**, 744–757.

Jorgensen, D. P., T. Matejka, and J. D. DuGranrut, 1996: Multi-beam techniques for deriving wind fields from airborne Doppler radars. *Meteor. Atmos. Phys*., **59**, 83-104.

Jorgensen, D. P., T. R. Shepherd, and A. Goldstein, 2000: A multiple pulse repetition frequency scheme for extending the unambiguous Doppler velocity of the NOAA P-3 airborne Doppler radar. *J. Atmos. Oceanic Techol*., **17**, 585-594.

Leise, J. A., 1981: A multidimensional scale-telescoped filter and data extension package. NOAA Tech. Memo. ERL WPL-82, 18 pp, (NTIS PB82-164104).

O'Brien, J. J., 1970: Alternative solutions to the classical vertical velocity problem. *J. Appl. Meteor*., **9**, 197-203.

Oye, R., R. C. Mueller, and S. Smith, 1995: Software for radar translation, visualization, editing, and interpolation. *Preprints, 27th Conf. on Radar Meteorology*, Vail, CO, Amer. Meteor. Soc., 359–364.

Rotunno, R., J. B. Klemp and M. L. Weisman, 1988: A theory for strong, long-lived squall lines. *J. Atmos. Sci*., **45**, 463--485.

Tessendorf, S.A. and R.J. Trapp, 2000: On the climatological distribution of tornadoes within quasi-linear convective systems. *Preprints, 20th Conf. on Severe Local Storms*, Orlando, Fl., Amer. Meteor. Soc., 134-137.

Weisman, M.L. and C. Davis, 1998: Mechanisms for the generation of mesoscale vortices within quasi-linear convective systems. *J. Atmos. Sci*., **55**, 2603-2622.